ORIGINAL PAPER

Mechanical stretch–induced endoplasmic reticulum stress, apoptosis and inflammation contribute to thoracic aortic aneurysm and dissection

Li-Xin Jia, Wen-Mei Zhang, Hong-Jia Zhang, Tao-Tao Li, Yue-Li Wang, Yan-Wen Qin, Hong Gu* and Jie Du*

Beijing Anzhen Hospital, Capital Medical University, Key Laboratory of Remodelling-related Cardiovascular Diseases, Ministry of Education, Beijing Collaborative Innovation Centre for Cardiovascular Disorders, Beijing Institute of Heart, Lung and Blood Vessel Disease, Beijing, People's Republic of China

*Correspondence to: H Gu and J Du, 2 Anzhen Road, Chaoyang District, Beijing Anzhen Hospital, Capital Medical University, Beijing Institute of Heart, Lung and Blood Vessel Disease, Beijing 100029, People's Republic of China. E-mail: koko_gu@hotmail.com and jdu@bcm.edu

Abstract

Thoracic aortic aneurysm/dissection (TAAD) is characterized by excessive smooth muscle cell (SMC) loss, extra-cellular matrix (ECM) degradation and inflammation. In response to certain stimuli, endoplasmic reticulum (ER) stress is activated and regulates apoptosis and inflammation. Excessive apoptosis promotes aortic inflammation and degeneration, leading to TAAD. Therefore, we studied the role of ER stress in TAAD formation. A lysyl oxidase inhibitor, 3-aminopropionitrile fumarate (BAPN), was administrated to induce TAAD formation in mice, which showed significant SMC loss (α-SMA level). Excessive apoptosis (TUNEL staining) and ER stress (ATF4 and CHOP), along with inflammation, were present in TAAD samples from both mouse and human. Transcriptional profiling of SMCs after mechanical stress demonstrated the expression of genes for ER stress and inflammation. To explore the causal role of ER stress in initiating degenerative signalling events and TAAD, we treated wild-type ($CHOP^{+/+}$) or $CHOP^{-/-}$ mice with BAPN and found that $CHOP$ deficiency protected against TAAD formation and rupture, as well as reduction in α-SMA level. Both SMC apoptosis and inflammation were significantly reduced in $CHOP^{-/-}$ mice. Moreover, SMCs isolated from $CHOP^{-/-}$ mice were resistant to mechanical stress-induced apoptosis. Taken together, our results demonstrated that mechanical stress-induced ER stress promotes SMCs apoptosis, inflammation and degeneration, providing insight into TAAD formation and progression.
© 2015 The Authors. *The Journal of Pathology* published by John Wiley & Sons Ltd on behalf of Pathological Society of Great Britain and Ireland.

Keywords: thoracic aortic aneurysm/dissection; SMCs; apoptosis; ER stress; CHOP

Introduction

Aortic aneurysm and dissection represents a major disease process affecting the aorta [1]. Thoracic aortic aneurysm/dissection (TAAD) has high mortality and the first symptom in up to 95% of patients is death with severe pain [1]. As there is no effective preventive therapy for TAAD, elucidation of the pathological mechanism(s) underlying aortic dissection is important for the development of new therapeutic treatments. TAAD is pathologically associated with degeneration of the aortic media, which is characterized by smooth muscle cell (SMC) loss, inflammation, fragmentation and depletion of elastic fibres [2,3]. As a key structural component of the aorta, SMCs play multiple roles in maintaining its function. In addition to their contractile function, SMCs continuously synthesize and degrade the extracellular matrix (ECM) and maintain its homeostasis [4]. Moreover, vascular wall SMCs sense haemodynamic

stress, leading to both cytoskeletal and ECM remodelling [5]. Apoptosis of SMCs has been observed in human TAAD specimens and is associated with TAAD progression [3,6]. However, the signalling pathways that trigger SMC apoptosis during the development of TAAD remain unclear.

Endoplasmic reticulum (ER) stress plays an important role in pathological vascular remodelling in cardiovascular diseases [7,8]. ER stress is characterized by signal transduction, triggered by the unfolded protein response (UPR). Three upstream signalling pathways constitute an ER-specific UPR, including the IRE1α–XBP1, ATF6 and PERK–eIF2–ATF4 pathways, but all three can transcriptionally regulate C/EBP homologous protein (CHOP) [9]. As a specific player in the UPR, the transcription factor CHOP (also known as GADD153 and DDIT3) initiates apoptotic events in the setting of severe or prolonged ER stress [10]. The role of CHOP in ER stress-induced apoptosis has been established in

atherosclerosis [10,11]. However, there is no direct evidence regarding whether ER stress is activated and how this might contribute to TAAD.

In this study, we aimed to determine the significance of ER stress in regulating TAAD *in vivo*. We found increased ER stress, SMC apoptosis and inflammation in both mouse model and human TAAD specimens. In a murine model of 3-aminopropionitrile fumarate (BAPN)-induced TAAD, *CHOP* deletion prevented SMC apoptosis, inflammation and TAAD incidence.

Materials and and methods

Patient specimens

Aneurysm samples were collected from TAAD patients in Beijing Anzhen Hospital who underwent repair surgery. None of the patients had a known genetic syndrome related to aortic disease, such as Marfan's, Turner's, Loeys–Dietz, or Ehlers–Danlos syndromes. Normal aorta samples were obtained from heart transplantation donors as described previously [12]. All protocols involving human specimens were approved by the Institutional Review Board of Beijing Anzhen Hospital, with each subject providing written informed consent, as described elsewhere [12] .

Animal model and ethics statement

Wild-type littermates ($CHOP^{+/+}$) and knockout ($CHOP^{-/-}$) mice on a C57B/L6 background were obtained from the Jackson Laboratory (Bar Harbor, ME, USA, stock no. 005530). The Institutional Animal Care and Use Committee of Capital Medical University, Beijing, China, approved all studies. The investigation conformed to the *Guide for the Care and Use of Laboratory Animals*, published by the US National Institutes of Health (NIH). Three week-old male mice were fed a normal diet and administered freshly prepared BAPN (Sigma-Aldrich, St. Louis, MO, USA) solution dissolved in the drinking water (1 g/kg/day) for 4 weeks, as described previously [13], with modifications.

Aortic ultrasonography monitoring

Mice were anaesthetized with 1% isoflurane and underwent echography in M-mode, using a high-resolution micro-ultrasound system (Vevo 2100, VisualSonics, Toronto, Canada) equipped with a 30 MHz transducer. Colour Doppler examination was performed to detect arterial flow.

Histology and immunohistochemistry

Mouse aorta and human specimens were fixed in 10% formalin, embedded in paraffin and sectioned at 5 μm thickness. Immunohistochemical staining was performed as described elsewhere [14,15]. Briefly, sections were treated with xylene to remove the paraffin and were rehydrated, incubated with 3% H_2O_2 for 10 min at room temperature and washed three times with phosphate-buffered saline (PBS). Then the sections were blocked with serum for 30 min and incubated with primary antibodies against ATF4 (Abcam, Cambridge, MA, USA; 1:200 dilution), proliferating cell nuclear antigen (PCNA; Abcam; 1:200 dilution), α-smooth muscle actin (α-SMA; Sigma; 1:500 dilution), CHOP (Santa Cruz Biotechnology, CA, and Cell Signaling Technology, Danvers, USA; 1:200 dilution), cleaved-caspase 3 (Cell Signaling Technology; 1:300 dilution), F4/80 (Abcam; 1:100 dilution), Mac-2 (Santa Cruz; 1:200 dilution) and immunoglobulin G (IgG) control (Santa Cruz), then the sections were incubated with the ChemMate™ EnVision™ System (Dako, Glostrup, Denmark). Images were captured and further analysed using ImageProPlus 3.0 (ECIPSE80i/90i).

For cryostat sections, mouse aorta samples were fixed in 4% paraformaldehyde, embedded in optimum cutting temperature (OCT) compound, frozen in liquid nitrogen and stored at −80 °C until sectioning. Apoptotic cells were identified using DeadEnd Fluorometric TUNEL (Promega, Madison, WI). TUNEL and α-SMA or F4/80 double staining was performed to detect apoptotic SMCs or apoptotic macrophages before confocal fluorescence microscopy analysis (Leica Microsystems, Buffalo Grove, IL, USA).

Elastin staining

Elastin fragmentation was graded based on the degree of elastin filament breakage, as described previously [14,16], with minor modifications. Elastin in the grafted veins was stained with the Gomrori's aldehyde-fuchsin staining method, using an elastic fibre staining kit (Maixin Bio, Fuzhou, China). Briefly, after deparaffinization and rehydration, sections were incubated for 5 min in Lugol's iodine solution, washed with PBS and incubated with sodium thiosulphate for 5 min. After washing with PBS and 70% ethanol, the sections were incubated with aldehyde-fuchsin for 10 min and acid Orange G for seconds.

Quantitative real-time PCR

Total RNA was extracted from thoracic aorta samples or cultured SMCs using Trizol reagent (Invitrogen, Carlsbad, CA, USA) and 2 μg was reversed-transcribed using the GoScript™ Reverse Transcription System (Promega), according to the manufacturer's instructions. For real-time quantitative PCR, the iQ5 system (Bio-Rad, Hercules, CA, USA) with SYBR Green I (Takara, Shiga, Japan) was used. Amplification was performed at 95 °C for 5 min, 95 °C for 45 s and 60 °C for 1 min of each step for 45 cycles. The housekeeping gene glyceraldehyde 3-phosphate dehydrogenase (*GAPDH*) was used as a control. The primers used are shown in Table S1 (see supplementary material).

Western blot analysis

Mouse aortae or cultured SMCs were harvested, snap-frozen in liquid nitrogen and stored at −80 °C. Protein was extracted using a Protein Extraction Kit containing protease inhibitor and Protein Phosphatase Inhibitor Cocktail. Equal amounts of protein extract (40 µg/lane) were separated using a 10% SDS–PAGE gel. The blot was further probed with the primary antibodies anti-GAPDH (1:2000 dilution; Sigma-Aldrich), anti-α-SMA (1:1000 dilution) and anti-CHOP (1:1000 dilution), then with IR dye-conjugated secondary antibodies (1:5000; Rochland Immunochemicals, Gilbertsville, PA, USA) for 1 h. The blots were then washed, exposed and analysed using an Odyssey infrared imaging system (LI-COR Biosciences Lincoln, NE, USA).

SMC culture, cyclic stretching and flow cytometry

SMCs were isolated from CHOP$^{+/+}$ and CHOP$^{-/-}$ mice, as described [17]. In brief, each mouse was euthanized by intraperitoneal injection of sodium pentobarbital. The aorta was removed and then digested with type II collagenase at 37 °C for 30 min to remove the adventitia. Then the endothelium was removed by gently rubbing the intima with a sterile cotton-tipped applicator, followed by a further digestion with a mixture of collagenase and elastase for 30 min. Cells were then cultured in Dulbecco's modified Eagle's medium (DMEM; Gibco) supplemented with 10% fetal bovine serum (FBS) and 1% penicillin–streptomycin. For cyclic stretching of SMCs, cells were cultured on silicone, elastomer-bottomed, collagen-coated plates (Flexcell, Hillsborough, NC, USA) at 37 °C overnight, then subjected to cyclic mechanical stretching, using a computer-controlled mechanical strain unit (Flexcell 5000) at a condition of 18% elongation, as described [18]. Apoptosis was detected by flow cytometry, using an Annexin V apoptosis detection kit (eBioscience, San Diego, CA, USA), following the manufacturer's protocol. For cytokine stimulation, SMCs were incubated with recombinant human IL-1β (rhIL-1β; R&D, Minneapolis, MN, USA) for 24 h at the indicated concentrations.

Statistical analysis

In all cases, the results from at least three independent experiments were used to calculate mean ± SD. Student's t-test was used for statistical analysis, and $p < 0.05$ was considered statistically significant.

Results

BAPN administration induced TAAD formation, showing SMCs loss and inflammation

It has been reported that lysyl oxidase (LOX), which crosslinks tropoelastin monomers to form elastic fibres,

plays a crucial role in regulating ECM homeostasis [19]. Inactivation of the *LOX* gene leads to aortic aneurysm and perinatal death in mice [20]. Administration of BAPN, a *LOX* inhibitor, along with angiotensin II infusion, causes aneurysm formation [13,21]. Failure of collagen crosslinking leads to loss of tensile strength of the aortic wall, subjecting the vascular wall to elevated vascular wall mechanical stress. Thus, BAPN is a model to study the pathogenesis of mechanical stress-induced aortic aneurysm. BAPN treatment induced TAAD formation when administered to 3 week-old mice. In 18 BAPN-treated mice, 16 developed TAAD and 10 of these died from rupture (Figure 1A–C). Haematixylin and eosin (H&E) and Van Gieson (VG) staining showed disarray of SMCs and elastin degradation after BAPN administration (Figure 1D). Both immunohistochemical staining and western blot were used to detect α-SMA. As shown in Figure 1E, F, the α-SMA level was significantly decreased after BAPN treatment. Macrophage infiltration and cytokine production were used to document vascular inflammation. BAPN administration significantly increased the infiltration of Mac-2-positive cells and of interleukin (IL-1β, IL-6) and chemokine (C–C motif) ligand 2 (*CCL2*) mRNA levels (Figure 1G, H).

SMCs apoptosis and ER stress are present after TAAD formation

It is known that SMC apoptosis contributes to SMC loss and TAAD formation. Previous studies have demonstrated that haemodynamic and mechanical stress is associated with TAAD development [4] and cyclic stretching induces SMC apoptosis, as well as ER stress *in vitro* [22]. We thus detected apoptosis by performing TUNEL staining and cleaved caspase-3 staining and found that apoptosis in the aortic wall was significantly increased in response to BAPN administration (Figure 2A, B). In a time-course study, apoptosis appeared at day 10 after BAPN treatment, according to TUNEL staining (see supplementary material, Figure S1A). Co-staining of TUNEL with α-SMA or F4/80 showed that the apoptotic cells were primarily SMCs (see supplementary material, Figure S1B); note that there were no macrophages (F4/80-positive cells) even at day 14. We then examined when macrophage infiltration occurred; as shown in Figure S1C (see supplementary material), macrophage infiltration in BAPN-treated mouse aorta appeared at the media area in the aorta on day 21 after BAPN administration, when TAAD appeared. These results suggest that SMC apoptosis is important for TAAD formation.

To link ER stress with TAAD, we measured the expression of ER stress-related genes in both mouse aorta and TAAD samples. The mRNA levels of both *ATF4* and *CHOP* were significantly up-regulated in TAAD samples, while the levels of *ATF6* and *GRP78* were not significantly changed (Figure 2C). Immunohistochemical staining showed that the levels of both
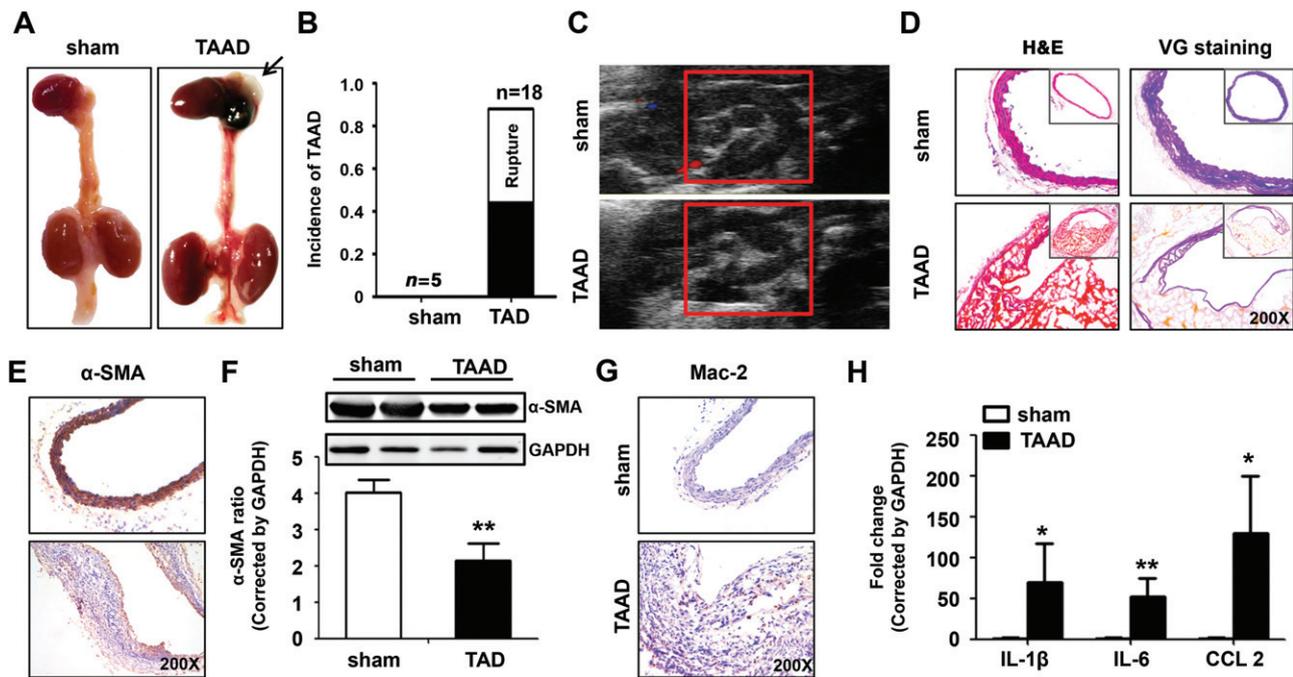
Figure 1. BAPN administration-induced TAAD formation, showing SMCs loss and inflammation in mice. (A) Representative images showed macroscopic features of isolated mouse aortae after saline or BAPN treatment for 28 days; arrow, location of TAAD. (B) Incidence of TAAD formation and rupture after BAPN administration. (C) Echography, showed aortic aneurysm formation in the arch of the thoracic aorta. (D) Haematoxylin and eosin (H&E) and elastic Van Gieson (VG) staining, showing cell disarray and elastin fragmentation after BAPN treatment. (E) Immunohistochemical staining. (F) Western blot analysis for α-SMA in mouse aortae from the sham and TAAD groups. (G) Imunohistochemical staining of Mac-2. (H) Quantitative RT–PCR (qRT–PCR) of mouse aortae ($n = 4$ in sham group, $n = 6$ in TAAD group); *$p < 0.05$, **$p < 0.01$ TAAD versus sham group

ATF4 and CHOP were higher in the dissection area (Figure 2D).

During TAAD development, the thoracic aorta loses tensile strength and is subjected to elevated mechanical stress. Studies have shown that, compared to the ascending aorta, SMC apoptosis increased at the aortic convexity during TAAD, where there was the highest stress [23]. Therefore, we treated SMCs with mechanical stretching (18% elongation for 2 h) and performed a microarray to explore how mechanical stress altered gene expression. Levels of GRP78, ATF4 and CHOP, as well as inflammation-related chemokines and cytokines, were up-regulated after mechanical stretch (Table 1). To examine the role of inflammation in ER stress and TAAD, ER stress was measured as the expression of CHOP in SMCs treated with mechanical stretching or IL-1β. Similar to mechanical stretching, IL-1β stimulated *CHOP* up-regulation in SMCs (Figure 2E).

Apoptosis, ER stress and inflammation were present in human TAAD specimens

To further confirm the pathological features of TAAD formation, human aorta samples with or without TAAD were evaluated. TUNEL staining and cleaved caspase-3 staining showed more apoptosis in TAAD patients than in the normal aorta (Figure 3A, B). To link ER stress with TAAD formation in human specimens, we showed that expression of ATF4 or CHOP was elevated in SMCs of human TAAD samples (Figure 3C, D). As prolonged

ER stress triggers caspase-dependent apoptosis [24], we performed co-staining of CHOP and cleaved caspase-3 and found that double-positive cells were present in human TAAD specimens (Figure 3E).

Knockout of CHOP, a mediator of ER stress, prevents TAAD formation

To demonstrate a causal role of CHOP-dependent signalling in TAAD development, both *CHOP*^{+/+} and *CHOP*^{−/−} mice were subjected to BAPN administration. The *CHOP*^{+/+} mice showed a higher incidence of TAAD formation (24/30) and rupture (11/24 TAADs) after BAPN administration, while *CHOP*^{−/−} mice had a much lower incidence of both TAAD formation (6/16) and rupture (1/6 TAADs) (Figure 4A–C). Moreover, the wall thickness was much thinner in *CHOP*^{−/−} than in *CHOP*^{+/+} mice (Figure 4D). The severity of TAAD was evaluated by elastin degradation grading (Figure 4E, upper panel) and *CHOP* deficiency prevented elastin degradation. Thus, *CHOP* deficiency significantly suppressed BAPN-induced TAAD formation. We next examined SMC loss by both immunohistochemical staining (Figure 4F) and western blot analysis (Figure 4H), and found that deficiency of *CHOP* prevented the loss of α-SMA after BAPN administration. However, PCNA staining showed no difference in cell proliferation between *CHOP*^{+/+} and *CHOP*^{−/−} mice (Figure 4G).
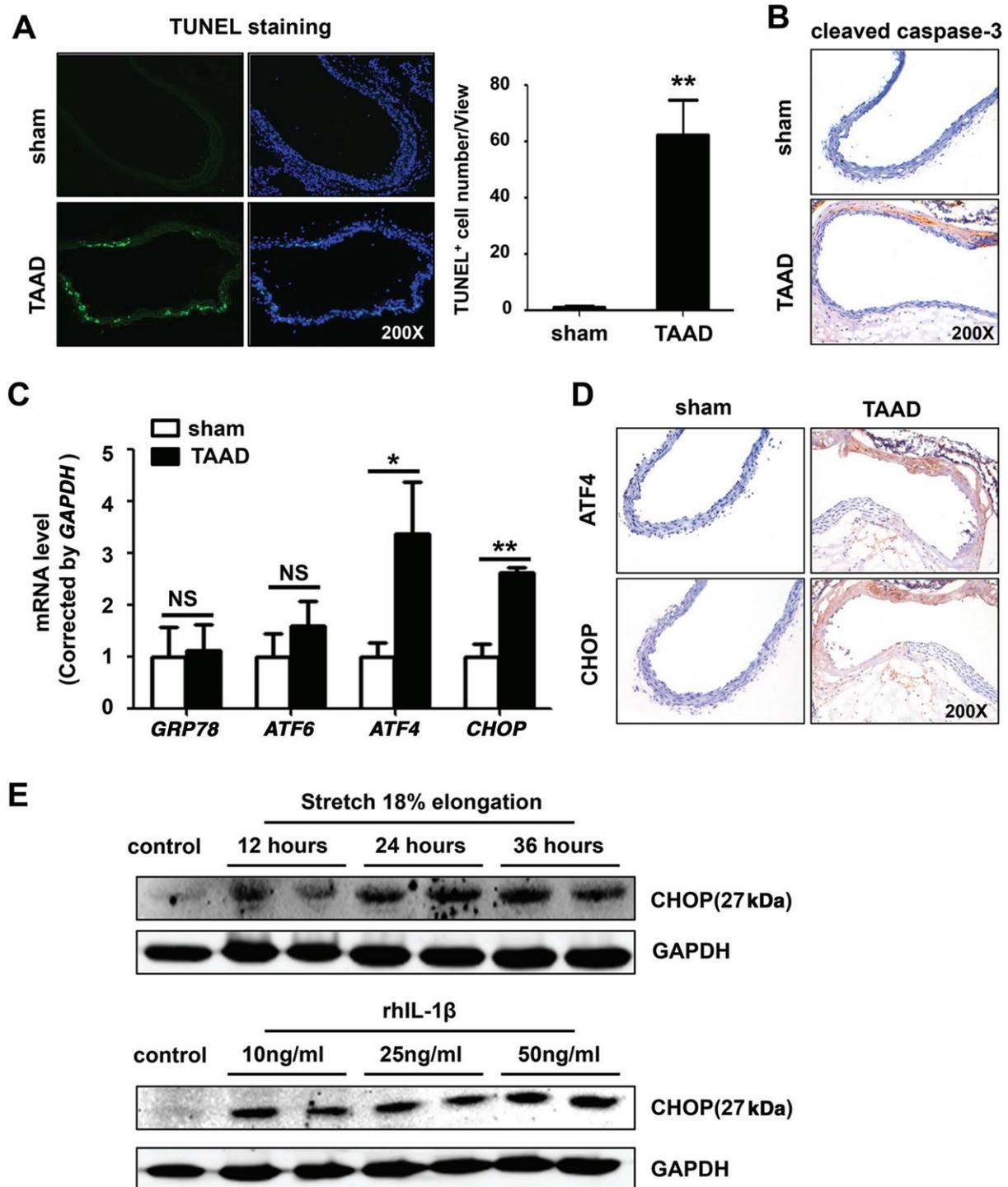
Figure 2. BAPN administration induced apoptosis and ER stress. (A) TUNEL and quantitation of sham- and BAPN-treated aortae ($n = 4$ in sham group, $n = 6$ in TAAD group). (B) Immunohistochemical staining for cleaved caspase-3. (C) Expression of ER stress-related genes, analysed by quantitative RT–PCR ($n = 4$ in sham group, $n = 6$ in TAAD group); $*p < 0.05$, $**p < 0.01$ TAAD versus sham group. (D) Representative immunohistochemical staining showed the expression of ATF4 and CHOP in sham- and BAPN-treated aortae. (E) Western blot analysis of CHOP expression in cultured mouse aorta SMCs treated with either mechanical stretch or rhIL-1β

CHOP deficiency suppresses SMC apoptosis in TAAD

ER transmembrane receptors detect the onset of ER stress and initiate the UPR to restore ER function, and prolonged ER stress induces CHOP transcription and initiates apoptosis [24]. As SMC apoptosis is associated with medial expansion and contributes to aortic aneurysm and dissection formation [25], we examined the consequence of CHOP-dependent ER stress and apoptosis in TAAD. CHOP$^{-/-}$ mice had fewer TUNEL-positive cells and smaller cleaved caspase-3-positive areas compared to CHOP$^{+/+}$ mice after BAPN administration (Figure 5A, B). In TAAD development, macrophages serve as the main source of MMPs production, which play a key role in ECM

Table 1. Mechanical stretch-induced up-regulated genes in SMCs

Gene name	Gene identifier	Ratio (linear)
Inflammation-related genes		
CXCL2	NM_053647	3.45
CXCL3	U22414	2.08
CXCL7	BF419899	1.58
CXCL9	AI169984	5.94
CCR2	AI707080	3.45
IL-6	NM_012589	7.17
IL-11	NM_133519	5.07
IL-16	AI137163	1.69
IL-23	NM_130410	5.94
ER stress-related genes		
GRP78	M14050	1.65
ATF4	NM_024403	1.80
CHOP	NM_024134	2.48

degradation, leading to TAAD formation [26]. To further confirm the cellular type of apoptotic cells in TAAD, we then performed co-staining of TUNEL with α-SMA or F4/80 to identify apoptotic SMCs or apoptotic macrophages. As is shown in Figure 5C, most TUNEL-positive cells were α-SMA-positive, while only a few TUNEL-positive cells were F4/80-positive (see supplementary material, Figure S2). Moreover, flow cytometry showed that mechanical stress induced SMC apoptosis *in vitro*, while *CHOP* deficiency prevented this effect (Figure 5D).

CHOP deficiency suppresses inflammation in TAAD

We next examined the role of CHOP in inflammation and MMP production. Both F4/80 staining and Mac-2 staining were used to track macrophages; there were significantly fewer positive cells in *CHOP*$^{-/-}$ than in *CHOP*$^{+/+}$ mice after BAPN administration (Figure 6A, B). The mRNA levels of *IL-1*β, *IL-6* and *CCL2* were

also decreased in *CHOP*$^{-/-}$ mice after BAPN treatment (Figure 6C). MMP-2 and MMP-9 production was also inhibited by *CHOP* deficiency in response to BAPN administration (Figure 6D, E).

Discussion

TAAD is pathologically associated with degeneration of the aortic media, which is characterized by SMC loss, along with fragmentation and depletion of elastic fibres [26]. SMC apoptosis has been observed and associated with the progression of TAAD. However, the signalling pathway that triggers SMC apoptosis in TAAD remains unclear. In this study, we demonstrated that inhibition of ER stress protected against SMCs apoptosis and inflammation, thereby preventing TAAD development.

Inflammatory cell infiltration and apoptotic cells have been reported in human specimens from thoracic aneurysm and dissection [3]. Consistent with this, our results showed that the mRNA levels of apoptosis- and inflammation-related genes were significantly increased in TAAD samples. Importantly, our results showed that ER stress was involved in TAAD development through regulating SMC apoptosis. Elevated mechanical stretching causes ER stress and inflammation in SMCs. Inflammation could further stimulate ER stress in a feed-forward manner in TAAD development. Our results are consistent with several studies indicating a critical role of inflammation in aneurysm/dissection progression. A recent study showed that genetic deletion of either *IL-1*β or *IL-1* receptor decreased inflammatory cytokine and SMC loss as well as elastin degradation, and pharmacological inhibition of IL-1β decreased TAAD formation and
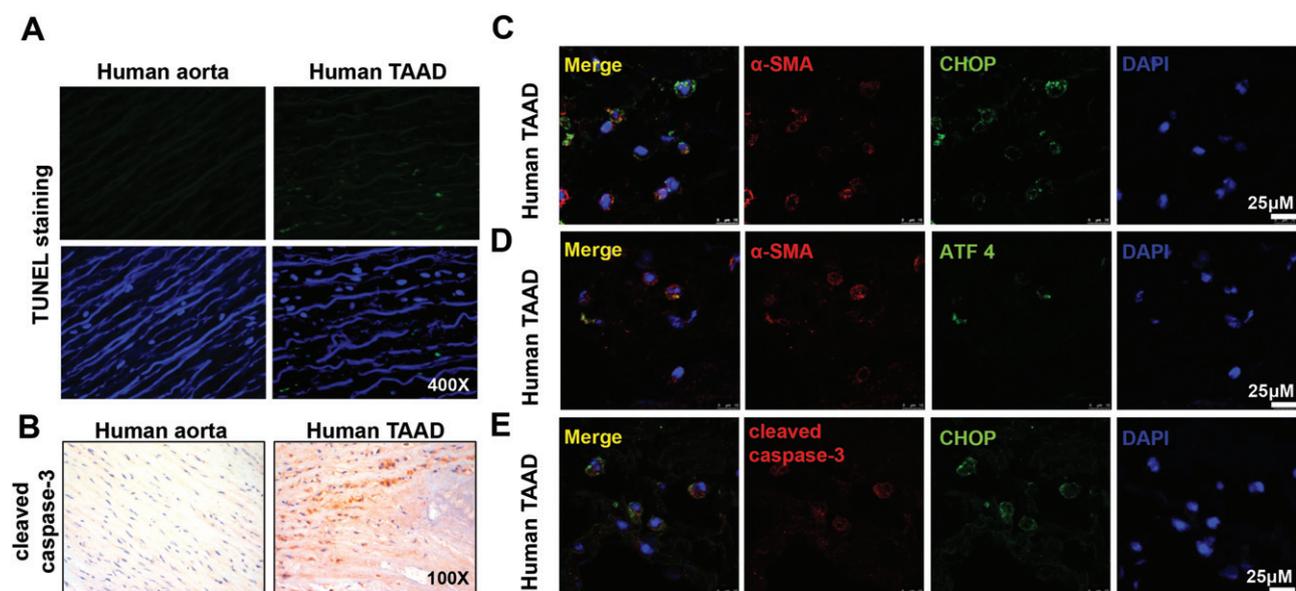
Figure 3. ER stress and cell apoptosis were present in human TAAD specimens. Representative pictures of (A) TUNEL and (B) cleaved caspase-3 on human normal aorta and TAAD samples. (C, D) ER stress-related proteins ATF4 and CHOP were co-stained with α-SMA. (E) Co-staining of cleaved caspase-3 and CHOP in human TAAD samples
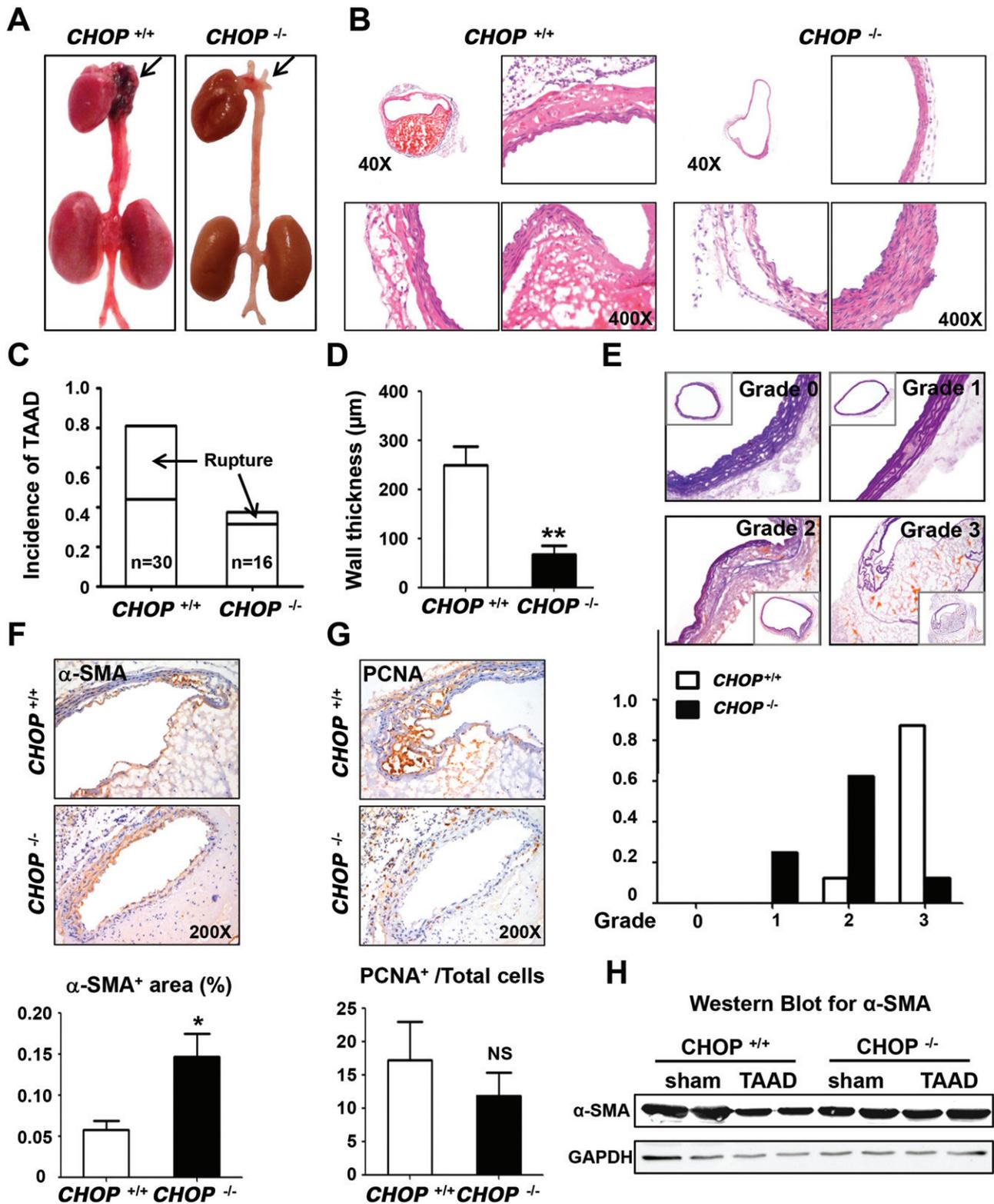
Figure 4. *CHOP* deficiency protected against BAPN administration-induced TAAD formation. (A) Representative photos of mouse aortae from *CHOP*^{+/+} and *CHOP*^{-/-} mice after BAPN treatment for 28 days. (B) Representative H&E staining of thoracic aortic dissections from *CHOP*^{+/+} and *CHOP*^{-/-} mice after BAPN treatment for 28 days. (C) Incidence of TAAD and rupture in *CHOP*^{+/+} and *CHOP*^{-/-} mice after BAPN administration. (D) Progression of thickening of the aortic media in *CHOP*^{+/+} and *CHOP*^{-/-} mice after BAPN treatment. (E) (Top) VG staining, showing elastin degradation grades: Grade 0, no degradation; Grade 1, mild degradation; Grade 2, severe degradation; Grade 4, dissection formation: (bottom) elastin degradation grades in CHOP^{+/+} and CHOP^{-/-} mice; **$p < 0.01$, CHOP^{+/+} versus CHOP^{-/-}, $n = 10$ in both groups. (F, G) Immunohistochemical staining for α-SMA and PCNA in CHOP^{+/+} and CHOP^{-/-} mice after BAPN administration; *$p < 0.05$, CHOP^{+/+} versus CHOP^{-/-}, $n = 6$ in both groups. (H) Western blot analysis of α-SMA expression in CHOP^{+/+} and CHOP^{-/-} mice with or without BAPN administration.
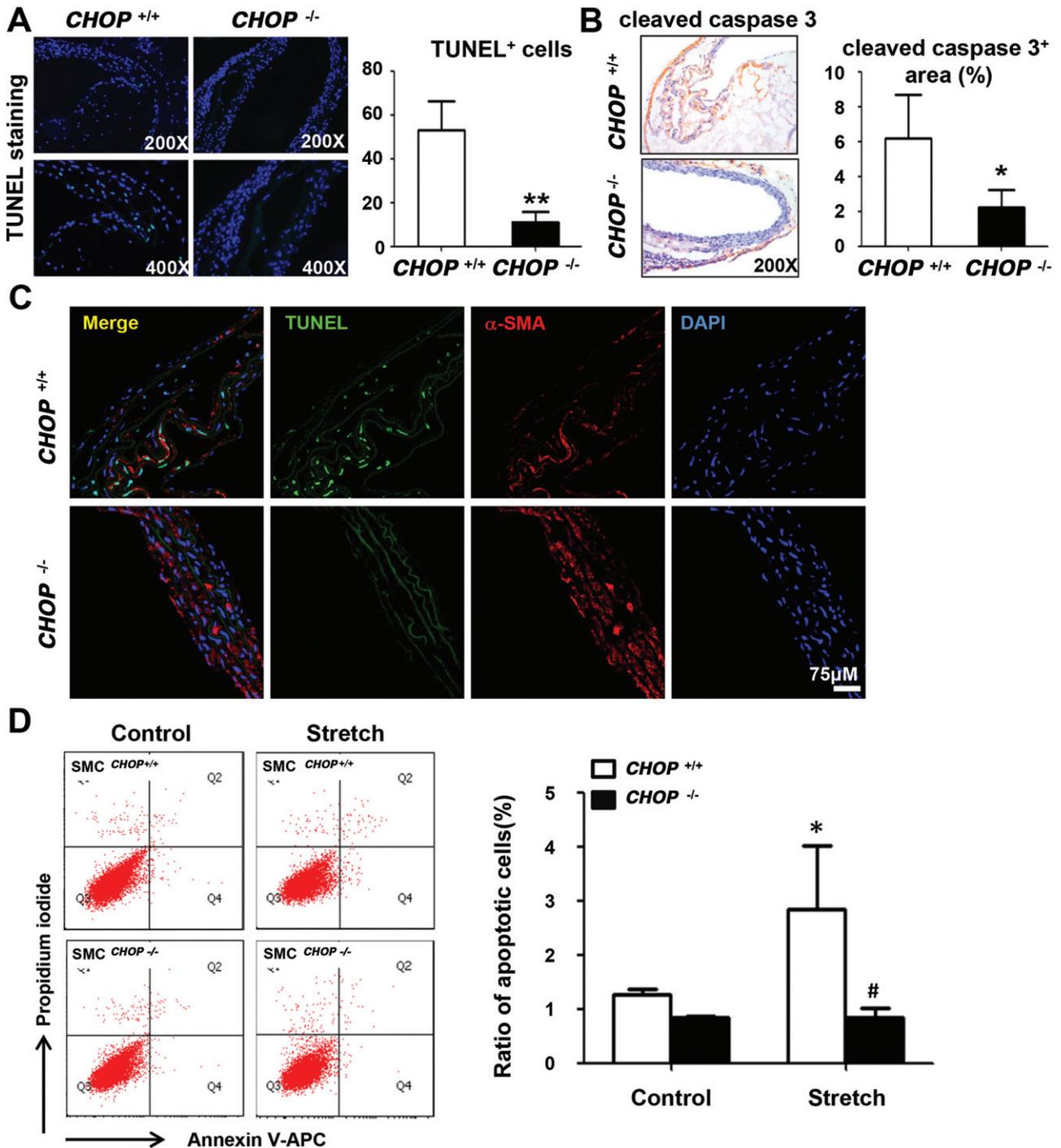
Figure 5. *CHOP* deficiency inhibited smooth muscle cell apoptosis during TAAD development. (A) Representative TUNEL and (B) cleaved caspase-3 staining in aortae from BAPN-treated *CHOP*+/+ and *CHOP*−/− mice; **$p < 0.01$, CHOP+/+ versus CHOP−/−, $n = 6$ in both groups. (C) Co-staining of α-SMA (red) and TUNEL (green). (D) Flow-cytometry analysis of propidium iodide and Annexin V of SMCs isolated from both *CHOP*+/+ and *CHOP*−/− mice and subjected to mechanical stretch for 36 h at 18% elongation; *$p < 0.05$, stretched SMCs from *CHOP*+/+ mice versus control *CHOP*+/+ SMCs; #$p < 0.05$, stretched SMCs from *CHOP*−/− mice versus stretched SMCs from *CHOP*+/+ mice; $n = 3$, repeated three times

progression [27]. Moreover, Tieu *et al* [28] reported that adventitial fibroblasts interact with infiltrated leukocytes to promote IL-6 production, inducing monocyte recruitment and activation, leading to MCP-1 secretion and TAAD formation in angiotensin II-infused aged mice. Regarding the role of inflammation and ER stress, it has also been reported that IL-1β can trigger ER stress and islet dysfunction [29].

ER stress primarily begins as a UPR for self-protection, while prolonged ER stress initiates cell apoptosis. The three signalling pathways activated during UPR (ie PERK, ATF6 and IRE1) involve switching from the adaptive response to apoptosis. UPR and/or ER-initiated apoptosis have been implicated in the pathophysiology of various cardiovascular diseases [30]. *CHOP*, also known as *GADD153* (growth
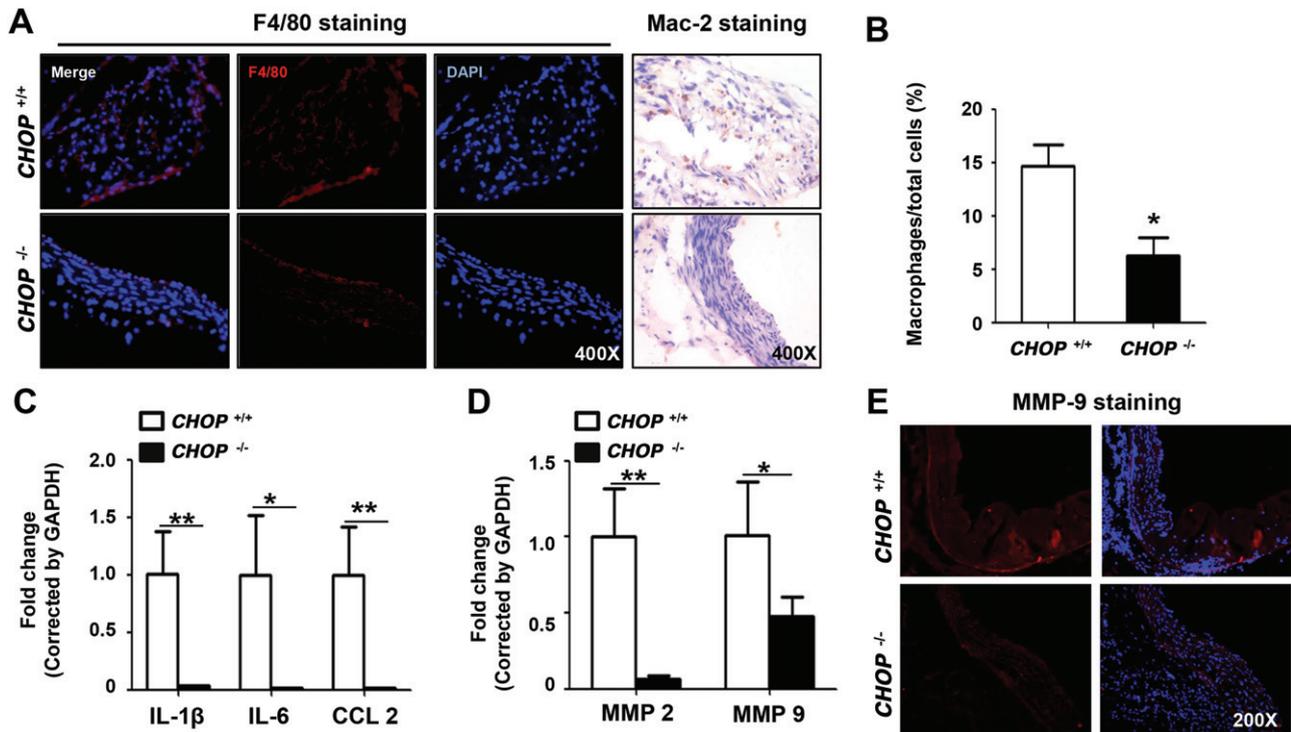
Figure 6. *CHOP* deficiency suppressed BAPN administration–induced inflammation and MMP production. (A) Immunostaining of macrophage markers, F4/80 and Mac-2, in BAPN-treated $CHOP^{+/+}$ and $CHOP^{-/-}$ mouse aortae. (B) Infiltrated macrophages in BAPN-treated mice ($n = 6$ in both groups); *$p < 0.05$, $CHOP^{+/+}$ versus $CHOP^{-/-}$ group. (C, D) mRNA levels of the indicated cytokines and MMPs by qRT–PCR ($n = 6$ in $CHOP^{+/+}$ group and $n = 5$ in $CHOP^{-/-}$ group); *$p < 0.05$, **$p < 0.01$, $CHOP^{+/+}$ versus $CHOP^{-/-}$. (E) Representative immunofluorescence staining of MMP-9 on sections from BAPN-treated $CHOP^{+/+}$ and $CHOP^{-/-}$ mouse aorta

arrest-and DNA damage inducible gene 153), is normally expressed at an undetectable level, but is markedly induced in response to various cellular stresses. CHOP has long been considered a proapoptotic factor of ER stress, which senses multiple stimuli, including mechanical stretching [31]. Moreover, the PERK–eIF2α–ATF4 pathway is essential for up-regulation of CHOP expression, albeit all three UPR-related pathways induce CHOP expression [24,32,33]. In this study, we showed that expression of CHOP, as well as the upstream ER stress factor ATF4, was induced in TAAD, thus establishing that ER stress and its signalling pathways are involved in TAAD development.

The existing mouse models for TAAD are mostly caused by genetic mutation, corresponding to specific familial TAAD syndomes, such as fibrillin-1 mutation, causing Marfan's syndrome, or *TGFβR* mutations, causing Loeys–Dietz syndrome [34]. In this study, we adopted a TAAD model using BAPN treatment (Figure 1), an inhibitor of *LOX*. LOX is a copper-dependent enzyme that initiates covalent crosslinking of elastin precursors by oxidizing peptidyl lysine to amino adipic semi-aldehydes. It has been reported that LOX plays a key role in vascular development by regulating ECM formation [20,35]. $LOX^{-/-}$ mice develop large aortic aneurysms, showing highly fragmented elastic fibres and discontinuity in the SMC layers [20]. Kurihara *et al* [13] reported that in mice with an FVB background treated with BAPN for 4 weeks, angiotensin II infusion for 24 h induced

TAAD rupture, but BAPN administration alone caused TAAD rupture in only about 20%. The present study showed a much higher incidence of TAAD formation and rupture in mice with a C57B/L6 background after BAPN treatment alone. This finding may be attributed to the different backgrounds, which have been shown to play different roles in several murine disease models [36,37]. Our data demonstrated that ER stress contributes to SMC apoptosis and TAAD formation, as *CHOP* deficiency significantly prevented the incidence of rupture after BAPN treatment (Figure 4).

SMCs are the principle cell type in the aorta, which is capable of matrix synthesis [38], protease or protease inhibitor elaboration [39] and inflammatory cell recruitment [40]. It is known that the central pathological characters are SMC loss and ECM degradation, resulting from an excess of proteases, including MMPs, cathepsins and elastase [26]. Apoptotic SMCs can initiate inflammation and enzyme secretion to promote TAAD development. Infiltrating inflammatory cells are also responsible for matrix destruction through secreting MMPs, including MMP-2 and MMP-9. Our results demonstrated that CHOP deficiency prevented SMC apoptosis both *in vivo* and *in vitro*, as well as inflammation (Figure 5). Prolonged ER stress initiates cell apoptosis through CHOP-, JNK- and caspase-12-dependent signalling pathways, and over-expression of CHOP leads to apoptosis [41,42]; therefore, CHOP induction initiates ER stress-induced cell apoptosis [31]. Our study showed that ATF4/CHOP

expression was present in parallel with the appearance of TUNEL-positive cells and cleaved caspase-3 production in both patients and mice (Figures 2, 3). Despite the obvious feature of SMC apoptosis in TAAD, SMC proliferation was also observed in the aorta [43]. The present data suggest that *CHOP* deficiency prevented SMC apoptosis and TAAD formation without affecting SMC proliferation (Figures 4, 5). Using an *in vitro* model of cyclic stretching-treated rat SMCs, cyclic stretching has been shown to increase CHOP expression and siRNA knockdown of CHOP in SMCs protected against mechanical stretch-induced cell apoptosis [22]. Consistent with these studies, our results demonstrate that elevated mechanical stretching induces CHOP expression, leading to SMC apoptosis, and promotes TAAD formation (Figures 4–6).

In conclusion, our present study identified that the ER stress effector CHOP is a key switch for SMC apoptosis, which promotes TAAD formation. The results of this study, together with recent findings showing induction of CHOP in response to cyclic stretching, suggest that the CHOP pathway may be a potential therapeutic target related to TAAD development.

Acknowledgements

Author contributions

LXJ, WMZ and TTL performed the experiments; YLW, YWQ and HG performed data analysis; HJZ prepared the human samples; and LXJ, HG and JD prepared the manuscript.

References

1. Elefteriades JA. Thoracic aortic aneurysm: reading the enemy's playbook. *Yale J Biol Med* 2008; **81:** 175–186.
2. Isselbacher EM. Thoracic and abdominal aortic aneurysms. *Circulation* 2005; **111:** 816–828.
3. He R, Guo DC, Estrera AL, *et al.* Characterization of the inflammatory and apoptotic cells in the aortas of patients with ascending thoracic aortic aneurysms and dissections. *J Thorac Cardiovasc Surg* 2006; **131:** 671–678.
4. El-Hamamsy I, Yacoub MH. Cellular and molecular mechanisms of thoracic aortic aneurysms. *Nat Rev Cardiol* 2009; **6:** 771–786.
5. Maniotis AJ, Chen CS, Ingber DE. Demonstration of mechanical connections between integrins, cytoskeletal filaments, and nucleoplasm that stabilize nuclear structure. *Proc Natl Acad Sci USA* 1997; **94:** 849–854.
6. Ihling C, Szombathy T, Nampoothiri K, *et al.* Cystic medial degeneration of the aorta is associated with p53 accumulation, Bax upregulation, apoptotic cell death, and cell proliferation. *Heart* 1999; **82:** 286–293.
7. Kitakaze M, Tsukamoto O. What is the role of ER stress in the heart? Introduction and series overview. *Circ Res* 2010; **107:** 15–18.
8. Minamino T, Komuro I, Kitakaze M. Endoplasmic reticulum stress as a therapeutic target in cardiovascular disease. *Circ Res* 2010; **107:** 1071–1082.
9. Ron D, Walter P. Signal integration in the endoplasmic reticulum unfolded protein response. *Nat Rev Mol Cell Biol* 2007; **8:** 519–529.
10. Thorp E, Li G, Seimon TA, *et al.* Reduced apoptosis and plaque necrosis in advanced atherosclerotic lesions of Apoe$^{-/-}$ and Ldlr$^{-/-}$ mice lacking CHOP. *Cell Metab* 2009; **9:** 474–481.
11. Tsukano H, Gotoh T, Endo M, *et al.* The endoplasmic reticulum stress–C/EBP homologous protein pathway-mediated apoptosis in macrophages contributes to the instability of atherosclerotic plaques. *Arterioscler Thromb Vasc Biol* 2010; **30:** 1925–1932.
12. Liu O, Jia L, Liu X, *et al.* Clopidogrel, a platelet P2Y12 receptor inhibitor, reduces vascular inflammation and angiotensin II induced-abdominal aortic aneurysm progression. *PLoS One* 2012; **7:** e51707.
13. Kurihara T, Shimizu-Hirota R, Shimoda M, *et al.* Neutrophil-derived matrix metalloproteinase 9 triggers acute aortic dissection. *Circulation* 2012; **126:** 3070–3080.
14. Shi HT, Wang Y, Jia LX, *et al.* Cathepsin S contributes to macrophage migration via degradation of elastic fibre integrity to facilitate vein graft neointimal hyperplasia. *Cardiovasc Res* 2014; **101:** 454–463.
15. Jia LX, Qi GM, Liu O, *et al.* Inhibition of platelet activation by clopidogrel prevents hypertension-induced cardiac inflammation and fibrosis. *Cardiovasc Drugs Ther* 2013; **27:** 521–530.
16. Qin Y, Cao X, Guo J, *et al.* Deficiency of cathepsin S attenuates angiotensin II-induced abdominal aortic aneurysm formation in apolipoprotein E-deficient mice. *Cardiovasc Res* 2012; **96:** 401–410.
17. Golovina VA, Blaustein MP. Preparation of primary cultured mesenteric artery smooth muscle cells for fluorescent imaging and physiological studies. *Nat Protoc* 2006; **1:** 2681–2687.
18. Wu X, Cheng J, Li P, *et al.* Mechano-sensitive transcriptional factor Egr-1 regulates insulin-like growth factor-1 receptor expression and contributes to neointima formation in vein grafts. *Arterioscler Thromb Vasc Biol* 2010; **30:** 471–476.
19. Rucker RB, Kosonen T, Clegg MS, *et al.* Copper, lysyl oxidase, and extracellular matrix protein crosslinking. *Am J Clin Nutr* 1998; **67:** 996–1002S.
20. Maki JM, Rasanen J, Tikkanen H, *et al.* Inactivation of the lysyl oxidase gene *Lox* leads to aortic aneurysms, cardiovascular dysfunction, and perinatal death in mice. *Circulation* 2002; **106:** 2503–2509.
21. Kurobe H, Matsuoka Y, Hirata Y, *et al.* Azelnidipine suppresses the progression of aortic aneurysm in wild mice model through anti-inflammatory effects. *J Thorac Cardiovasc Surg* 2013; **146:** 1501–1508.
22. Cheng WP, Hung HF, Wang BW, Shyu KG. The molecular regulation of GADD153 in apoptosis of cultured vascular smooth muscle cells by cyclic mechanical stretch. *Cardiovasc Res* 2008; **77:** 551–559.
23. Della Corte A, Quarto C, Bancone C, *et al.* Spatiotemporal patterns of smooth muscle cell changes in ascending aortic dilatation with bicuspid and tricuspid aortic valve stenosis: focus on cell-matrix signaling. *J Thorac Cardiovasc Surg* 2008; **135:** 8–18, 18e11–12.
24. Szegezdi E, Logue SE, Gorman AM, Samali A. Mediators of endoplasmic reticulum stress-induced apoptosis. *EMBO Rep* 2006; **7:** 880–885.
25. Clarke MC, Littlewood TD, Figg N, *et al.* Chronic apoptosis of vascular smooth muscle cells accelerates atherosclerosis and promotes calcification and medial degeneration. *Circ Res* 2008; **102:** 1529–1538.
26. Wu D, Shen YH, Russell L, *et al.* Molecular mechanisms of thoracic aortic dissection. *J Surg Res* 2013; **184:** 907–924.

27. Johnston WF, Salmon M, Pope NH, *et al.* Inhibition of interleukin-1β decreases aneurysm formation and progression in a novel model of thoracic aortic aneurysms. *Circulation* 2014; **130:** S51–59.

28. Tieu BC, Lee C, Sun H, *et al.* An adventitial IL-6/MCP1 amplification loop accelerates macrophage-mediated vascular inflammation leading to aortic dissection in mice. *J Clin Invest* 2009; **119:** 3637–3651.

29. O'Neill CM, Lu C, Corbin KL, *et al.* Circulating levels of IL-1B + IL-6 cause ER stress and dysfunction in islets from prediabetic male mice. *Endocrinology* 2013; **154:** 3077–3088.

30. Minamino T, Kitakaze M. ER stress in cardiovascular disease. *J Mol Cell Cardiol* 2010; **48:** 1105–1110.

31. Okada K, Minamino T, Tsukamoto Y, *et al.* Prolonged endoplasmic reticulum stress in hypertrophic and failing heart after aortic constriction: possible contribution of endoplasmic reticulum stress to cardiac myocyte apoptosis. *Circulation* 2004; **110:** 705–712.

32. Oyadomari S, Mori M. Roles of CHOP/GADD153 in endoplasmic reticulum stress. *Cell Death Differ* 2004; **11:** 381–389.

33. Xu C, Bailly-Maitre B, Reed JC. Endoplasmic reticulum stress: cell life and death decisions. *J Clin Invest* 2005; **115:** 2656–2664.

34. Lindsay ME, Dietz HC. Lessons on the pathogenesis of aneurysm from heritable conditions. *Nature* 2011; **473:** 308–316.

35. Andrews EJ, White WJ, Bullock LP. Spontaneous aortic aneurysms in blotchy mice. *Am J Pathol* 1975; **78:** 199–210.

36. Asano Y, Koishi K, Frugier T, McLennan IS. Mice with disrupted TGFβ signaling have normal cerebella development, but exhibit facial dysmorphogenesis and strain-dependent deficits in their body wall. *Cell Mol Neurobiol* 2009; **29:** 621–633.

37. van den Borne SW, van de Schans VA, Strzelecka AE, *et al.* Mouse strain determines the outcome of wound healing after myocardial infarction. *Cardiovasc Res* 2009; **84:** 273–282.

38. Koch AE, Haines GK, Rizzo RJ, *et al.* Human abdominal aortic aneurysms. Immunophenotypic analysis suggesting an immune-mediated response. *Am J Pathol* 1990; **137:** 1199–1213.

39. Pyo R, Lee JK, Shipley JM, *et al.* Targeted gene disruption of matrix metalloproteinase-9 (gelatinase B) suppresses development of experimental abdominal aortic aneurysms. *J Clin Invest* 2000; **105:** 1641–1649.

40. Leeper NJ, Tedesco MM, Kojima Y, *et al.* Apelin prevents aortic aneurysm formation by inhibiting macrophage inflammation. *Am J Physiol Heart Circ Physiol* 2009; **296:** H1329–1335.

41. Oyadomari S, Araki E, Mori M. Endoplasmic reticulum stress-mediated apoptosis in pancreatic β cells. *Apoptosis* 2002; **7:** 335–345.

42. Kaufman RJ. Stress signaling from the lumen of the endoplasmic reticulum: coordination of gene transcriptional and translational controls. *Genes Dev* 1999; **13:** 1211–1233.

43. Nagashima H, Sakomura Y, Aoka Y, *et al.* Angiotensin II type 2 receptor mediates vascular smooth muscle cell apoptosis in cystic medial degeneration associated with Marfan's syndrome. *Circulation* 2001; **104:** I282–287.

SUPPLEMENTARY MATERIAL ON THE INTERNET

The following supplementary material may be found in the online version of this article:

Figure S1. TUNEL and co-staining with SMCs and macrophages

Figure S2. TUNEL co-staining with F4/80 in $CHOP^{+/+}$ and $CHOP^{-/-}$ mouse aortae

Table S1. Primers used in this study

---

50 Years ago in the *Journal of Pathology...*

Histological studies and measurement of nucleic acid synthesis in rat mammary tumours induced by 9,10-dimethyl-1,2-benzanthracene (DMBA)

L. Stevens, Evelyn Stevens and A. R. Currie

To view these articles, and more, please visit:
www.thejournalofpathology.com

Click 'ALL ISSUES (1892 - 2015)', to read articles going right back to Volume 1, Issue 1.

The Journal of Pathology
Understanding Disease

Journal of
The Pathological Society